

Search for Resonant $t\bar{t}$ Production in $p\bar{p}$ Collisions at $\sqrt{s} = 1.96$ TeV

T. Aaltonen,²³ A. Abulencia,²⁴ J. Adelman,¹³ T. Akimoto,⁵⁴ M.G. Albrow,¹⁷ B. Álvarez González,¹¹ S. Amerio,⁴²
 D. Amidei,³⁴ A. Anastassov,⁵¹ A. Annovi,¹⁹ J. Antos,¹⁴ G. Apollinari,¹⁷ A. Apresyan,⁴⁷ T. Arisawa,⁵⁶ A. Artikov,¹⁵
 W. Ashmanskas,¹⁷ A. Attal,³ A. Aurisano,⁵² F. Azfar,⁴¹ P. Azzi-Bacchetta,⁴² P. Azzurri,⁴⁵ N. Bacchetta,⁴²
 W. Badgett,¹⁷ A. Barbaro-Galtieri,²⁸ V.E. Barnes,⁴⁷ B.A. Barnett,²⁵ S. Baroiant,⁷ V. Bartsch,³⁰ G. Bauer,³²
 P.-H. Beauchemin,³³ F. Bedeschi,⁴⁵ P. Bednar,¹⁴ S. Behari,²⁵ G. Bellettini,⁴⁵ J. Bellinger,⁵⁸ A. Belloni,³²
 D. Benjamin,¹⁶ A. Beretvas,¹⁷ J. Beringer,²⁸ T. Berry,²⁹ A. Bhatti,⁴⁹ M. Binkley,¹⁷ D. Bisello,⁴² I. Bizjak,³⁰
 R.E. Blair,² C. Blocker,⁶ B. Blumenfeld,²⁵ A. Bocci,¹⁶ A. Bodek,⁴⁸ V. Boisvert,⁴⁸ G. Bolla,⁴⁷ A. Bolshov,³²
 D. Bortoletto,⁴⁷ J. Boudreau,⁴⁶ A. Boveia,¹⁰ B. Brau,¹⁰ L. Brigliadori,⁵ C. Bromberg,³⁵ E. Brubaker,¹³
 J. Budagov,¹⁵ H.S. Budd,⁴⁸ S. Budd,²⁴ K. Burkett,¹⁷ G. Busetto,⁴² P. Bussey,²¹ A. Buzatu,³³ K. L. Byrum,²
 S. Cabrera^r,¹⁶ M. Campanelli,³⁵ M. Campbell,³⁴ F. Canelli,¹⁷ A. Canepa,⁴⁴ D. Carlsmith,⁵⁸ R. Carosi,⁴⁵
 S. Carrillo^l,¹⁸ S. Carron,³³ B. Casal,¹¹ M. Casarsa,¹⁷ A. Castro,⁵ P. Catastini,⁴⁵ D. Cauz,⁵³ M. Cavalli-Sforza,³
 A. Cerri,²⁸ L. Cerrito^p,³⁰ S.H. Chang,²⁷ Y.C. Chen,¹ M. Chertok,⁷ G. Chiarelli,⁴⁵ G. Chlachidze,¹⁷ F. Chlebana,¹⁷
 K. Cho,²⁷ D. Chokheli,¹⁵ J.P. Chou,²² G. Choudalakis,³² S.H. Chuang,⁵¹ K. Chung,¹² W.H. Chung,⁵⁸ Y.S. Chung,⁴⁸
 C.I. Ciobanu,²⁴ M.A. Ciocci,⁴⁵ A. Clark,²⁰ D. Clark,⁶ G. Compostella,⁴² M.E. Convery,¹⁷ J. Conway,⁷ B. Cooper,³⁰
 K. Copic,³⁴ M. Cordelli,¹⁹ G. Cortiana,⁴² F. Crescioli,⁴⁵ C. Cuenca Almenar^r,⁷ J. Cuevas^o,¹¹ R. Culbertson,¹⁷
 J.C. Cully,³⁴ D. Dagenhart,¹⁷ M. Datta,¹⁷ T. Davies,²¹ P. de Barbaro,⁴⁸ S. De Cecco,⁵⁰ A. Deisher,²⁸
 G. De Lentdecker^d,⁴⁸ G. De Lorenzo,³ M. Dell'Orso,⁴⁵ L. Demortier,⁴⁹ J. Deng,¹⁶ M. Deninno,⁵ D. De Pedis,⁵⁰
 P.F. Derwent,¹⁷ G.P. Di Giovanni,⁴³ C. Dionisi,⁵⁰ B. Di Ruzza,⁵³ J.R. Dittmann,⁴ M. D'Onofrio,³ S. Donati,⁴⁵
 P. Dong,⁸ J. Donini,⁴² T. Dorigo,⁴² S. Dube,⁵¹ J. Efron,³⁸ R. Erbacher,⁷ D. Errede,²⁴ S. Errede,²⁴ R. Eusebi,¹⁷
 H.C. Fang,²⁸ S. Farrington,²⁹ W.T. Fedorko,¹³ R.G. Feild,⁵⁹ M. Feindt,²⁶ J.P. Fernandez,³¹ C. Ferrazza,⁴⁵
 R. Field,¹⁸ G. Flanagan,⁴⁷ R. Forrest,⁷ S. Forrester,⁷ M. Franklin,²² J.C. Freeman,²⁸ I. Furic,¹⁸ M. Gallinaro,⁴⁹
 J. Galyardt,¹² F. Garberon,¹⁰ J.E. Garcia,⁴⁵ A.F. Garfinkel,⁴⁷ H. Gerberich,²⁴ D. Gerdes,³⁴ S. Giagu,⁵⁰
 P. Giannetti,⁴⁵ K. Gibson,⁴⁶ J.L. Gimmell,⁴⁸ C. Ginsburg,¹⁷ N. Giokaris^a,¹⁵ M. Giordani,⁵³ P. Giromini,¹⁹
 M. Giunta,⁴⁵ V. Glagolev,¹⁵ D. Glenzinski,¹⁷ M. Gold,³⁶ N. Goldschmidt,¹⁸ J. Goldstein^c,⁴¹ A. Golossanov,¹⁷
 G. Gomez,¹¹ G. Gomez-Ceballos,³² M. Goncharov,⁵² O. González,³¹ I. Gorelov,³⁶ A.T. Goshaw,¹⁶ K. Goulianos,⁴⁹
 A. Gresele,⁴² S. Grinstein,²² C. Grosso-Pilcher,¹³ R.C. Group,¹⁷ U. Grundler,²⁴ J. Guimaraes da Costa,²²
 Z. Gunay-Unalan,³⁵ C. Haber,²⁸ K. Hahn,³² S.R. Hahn,¹⁷ E. Halkiadakis,⁵¹ A. Hamilton,²⁰ B.-Y. Han,⁴⁸
 J.Y. Han,⁴⁸ R. Handler,⁵⁸ F. Happacher,¹⁹ K. Hara,⁵⁴ D. Hare,⁵¹ M. Hare,⁵⁵ S. Harper,⁴¹ R.F. Harr,⁵⁷
 R.M. Harris,¹⁷ M. Hartz,⁴⁶ K. Hatakeyama,⁴⁹ J. Hauser,⁸ C. Hays,⁴¹ M. Heck,²⁶ A. Heijboer,⁴⁴ B. Heinemann,²⁸
 J. Heinrich,⁴⁴ C. Henderson,³² M. Herndon,⁵⁸ J. Heuser,²⁶ S. Hewamanage,⁴ D. Hidas,¹⁶ C.S. Hill^c,¹⁰
 D. Hirschbuehl,²⁶ A. Hocker,¹⁷ S. Hou,¹ M. Houlden,²⁹ S.-C. Hsu,⁹ B.T. Huffman,⁴¹ R.E. Hughes,³⁸ U. Husemann,⁵⁹
 J. Huston,³⁵ J. Incandela,¹⁰ G. Introzzi,⁴⁵ M. Iori,⁵⁰ A. Ivanov,⁷ B. Iyutin,³² E. James,¹⁷ B. Jayatilaka,¹⁶
 D. Jeans,⁵⁰ E.J. Jeon,²⁷ S. Jindariani,¹⁸ W. Johnson,⁷ M. Jones,⁴⁷ K.K. Joo,²⁷ S.Y. Jun,¹² J.E. Jung,²⁷
 T.R. Junk,²⁴ T. Kamon,⁵² D. Kar,¹⁸ P.E. Karchin,⁵⁷ Y. Kato,⁴⁰ R. Kephart,¹⁷ U. Kerzel,²⁶ V. Khotilovich,⁵²
 B. Kilminster,³⁸ D.H. Kim,²⁷ H.S. Kim,²⁷ J.E. Kim,²⁷ M.J. Kim,¹⁷ S.B. Kim,²⁷ S.H. Kim,⁵⁴ Y.K. Kim,¹³
 N. Kimura,⁵⁴ L. Kirsch,⁶ S. Klimenko,¹⁸ M. Klute,³² B. Knuteson,³² B.R. Ko,¹⁶ S.A. Koay,¹⁰ K. Kondo,⁵⁶
 D.J. Kong,²⁷ J. Konigsberg,¹⁸ A. Korytov,¹⁸ A.V. Kotwal,¹⁶ J. Kraus,²⁴ M. Kreps,²⁶ J. Kroll,⁴⁴ N. Krumnack,⁴
 M. Kruse,¹⁶ V. Krutelyov,¹⁰ T. Kubo,⁵⁴ S. E. Kuhlmann,² T. Kuhr,²⁶ N.P. Kulkarni,⁵⁷ Y. Kusakabe,⁵⁶ S. Kwang,¹³
 A.T. Laasanen,⁴⁷ S. Lai,³³ S. Lami,⁴⁵ S. Lammel,¹⁷ M. Lancaster,³⁰ R.L. Lander,⁷ K. Lannon,³⁸ A. Lath,⁵¹
 G. Latino,⁴⁵ I. Lazzizzera,⁴² T. LeCompte,² J. Lee,⁴⁸ J. Lee,²⁷ Y.J. Lee,²⁷ S.W. Lee^q,⁵² R. Lefèvre,²⁰ N. Leonardo,³²
 S. Leone,⁴⁵ S. Levy,¹³ J.D. Lewis,¹⁷ C. Lin,⁵⁹ C.S. Lin,¹⁷ M. Lindgren,¹⁷ E. Lipeles,⁹ A. Lister,⁷ D.O. Litvintsev,¹⁷
 T. Liu,¹⁷ N.S. Lockyer,⁴⁴ A. Loginov,⁵⁹ M. Loreti,⁴² L. Lovas,¹⁴ R.-S. Lu,¹ D. Lucchesi,⁴² J. Lueck,²⁶ C. Luci,⁵⁰
 P. Lujan,²⁸ P. Lukens,¹⁷ G. Lungu,¹⁸ L. Lyons,⁴¹ J. Lys,²⁸ R. Lysak,¹⁴ E. Lytken,⁴⁷ P. Mack,²⁶ D. MacQueen,³³
 R. Madrak,¹⁷ K. Maeshima,¹⁷ K. Makhoul,³² T. Maki,²³ P. Maksimovic,²⁵ S. Malde,⁴¹ S. Malik,³⁰ G. Manca,²⁹
 A. Manousakis^a,¹⁵ F. Margaroli,⁴⁷ C. Marino,²⁶ C.P. Marino,²⁴ A. Martin,⁵⁹ M. Martin,²⁵ V. Martin^j,²¹
 M. Martínez,³ R. Martínez-Ballarín,³¹ T. Maruyama,⁵⁴ P. Mastrandrea,⁵⁰ T. Masubuchi,⁵⁴ M.E. Mattson,⁵⁷
 P. Mazzanti,⁵ K.S. McFarland,⁴⁸ P. McIntyre,⁵² R. McNultyⁱ,²⁹ A. Mehta,²⁹ P. Mehtala,²³ S. Menzemer^k,¹¹
 A. Menzione,⁴⁵ P. Merkel,⁴⁷ C. Mesropian,⁴⁹ A. Messina,³⁵ T. Miao,¹⁷ N. Miladinovic,⁶ J. Miles,³² R. Miller,³⁵
 C. Mills,²² M. Milnik,²⁶ A. Mitra,¹ G. Mitselmakher,¹⁸ H. Miyake,⁵⁴ S. Moed,²⁰ N. Moggi,⁵ C.S. Moon,²⁷
 R. Moore,¹⁷ M. Morello,⁴⁵ P. Movilla Fernandez,²⁸ J. Mülmenstädt,²⁸ A. Mukherjee,¹⁷ Th. Muller,²⁶ R. Mumford,²⁵

P. Murat,¹⁷ M. Mussini,⁵ J. Nachtman,¹⁷ Y. Nagai,⁵⁴ A. Nagano,⁵⁴ J. Naganoma,⁵⁶ K. Nakamura,⁵⁴ I. Nakano,³⁹ A. Napier,⁵⁵ V. Necula,¹⁶ C. Neu,⁴⁴ M.S. Neubauer,²⁴ J. Nielsen^f,²⁸ L. Nodulman,² M. Norman,⁹ O. Norniella,²⁴ E. Nurse,³⁰ S.H. Oh,¹⁶ Y.D. Oh,²⁷ I. Oksuzian,¹⁸ T. Okusawa,⁴⁰ R. Oldeman,²⁹ R. Orava,²³ K. Osterberg,²³ S. Pagan Griso,⁴² C. Pagliarone,⁴⁵ E. Palencia,¹⁷ V. Papadimitriou,¹⁷ A. Papaikonomou,²⁶ A.A. Paramonov,¹³ B. Parks,³⁸ S. Pashapour,³³ J. Patrick,¹⁷ G. Pauletta,⁵³ M. Paulini,¹² C. Paus,³² D.E. Pellett,⁷ A. Penzo,⁵³ T.J. Phillips,¹⁶ G. Piacentino,⁴⁵ J. Piedra,⁴³ L. Pinera,¹⁸ K. Pitts,²⁴ C. Plager,⁸ L. Pondrom,⁵⁸ X. Portell,³ O. Poukhov,¹⁵ N. Pounder,⁴¹ F. Prakoshyn,¹⁵ A. Pronko,¹⁷ J. Proudfoot,² F. Ptohos^h,¹⁷ G. Punzi,⁴⁵ J. Pursley,⁵⁸ J. Rademacker^c,⁴¹ A. Rahaman,⁴⁶ V. Ramakrishnan,⁵⁸ N. Ranjan,⁴⁷ I. Redondo,³¹ B. Reisert,¹⁷ V. Rekovic,³⁶ P. Renton,⁴¹ M. Rescigno,⁵⁰ S. Richter,²⁶ F. Rimondi,⁵ L. Ristori,⁴⁵ A. Robson,²¹ T. Rodrigo,¹¹ E. Rogers,²⁴ S. Rolli,⁵⁵ R. Roser,¹⁷ M. Rossi,⁵³ R. Rossin,¹⁰ P. Roy,³³ A. Ruiz,¹¹ J. Russ,¹² V. Rusu,¹⁷ H. Saarikko,²³ A. Safonov,⁵² W.K. Sakumoto,⁴⁸ G. Salamanna,⁵⁰ O. Saltó,³ L. Santi,⁵³ S. Sarkar,⁵⁰ L. Sartori,⁴⁵ K. Sato,¹⁷ P. Savard,³³ A. Savoy-Navarro,⁴³ T. Scheidle,²⁶ P. Schlabach,¹⁷ E.E. Schmidt,¹⁷ M.P. Schmidt,⁵⁹ M. Schmitt,³⁷ T. Schwarz,⁷ L. Scodellaro,¹¹ A.L. Scott,¹⁰ A. Scribano,⁴⁵ F. Scuri,⁴⁵ A. Sedov,⁴⁷ S. Seidel,³⁶ Y. Seiya,⁴⁰ A. Semenov,¹⁵ L. Sexton-Kennedy,¹⁷ A. Sfyrla,²⁰ S.Z. Shalhout,⁵⁷ M.D. Shapiro,²⁸ T. Shears,²⁹ P.F. Shepard,⁴⁶ D. Sherman,²² M. Shimojimaⁿ,⁵⁴ M. Shochet,¹³ Y. Shon,⁵⁸ I. Shreyber,²⁰ A. Sidoti,⁴⁵ P. Sinervo,³³ A. Sisakyan,¹⁵ A.J. Slaughter,¹⁷ J. Slaunwhite,³⁸ K. Sliwa,⁵⁵ J.R. Smith,⁷ F.D. Snider,¹⁷ R. Snihur,³³ M. Soderberg,³⁴ A. Soha,⁷ S. Somalwar,⁵¹ V. Sorin,³⁵ J. Spalding,¹⁷ F. Spinella,⁴⁵ T. Spreitzer,³³ P. Squillacioti,⁴⁵ M. Stanitzki,⁵⁹ R. St. Denis,²¹ B. Stelzer,⁸ O. Stelzer-Chilton,⁴¹ D. Stentz,³⁷ J. Strologas,³⁶ D. Stuart,¹⁰ J.S. Suh,²⁷ A. Sukhanov,¹⁸ H. Sun,⁵⁵ I. Suslov,¹⁵ T. Suzuki,⁵⁴ A. Taffard^e,²⁴ R. Takashima,³⁹ Y. Takeuchi,⁵⁴ R. Tanaka,³⁹ M. Tecchio,³⁴ P.K. Teng,¹ K. Terashi,⁴⁹ J. Thom^g,¹⁷ A.S. Thompson,²¹ G.A. Thompson,²⁴ E. Thomson,⁴⁴ P. Tipton,⁵⁹ V. Tiwari,¹² S. Tkaczyk,¹⁷ D. Toback,⁵² S. Tokar,¹⁴ K. Tollefson,³⁵ T. Tomura,⁵⁴ D. Tonelli,¹⁷ S. Torre,¹⁹ D. Torretta,¹⁷ S. Tourneur,⁴³ W. Trischuk,³³ Y. Tu,⁴⁴ N. Turini,⁴⁵ F. Ukegawa,⁵⁴ S. Uozumi,⁵⁴ S. Vallecorsa,²⁰ N. van Remortel,²³ A. Varganov,³⁴ E. Vataga,³⁶ F. Vázquez^l,¹⁸ G. Velev,¹⁷ C. Vellidis^a,⁴⁵ V. Veszpremi,⁴⁷ M. Vidal,³¹ R. Vidal,¹⁷ I. Vila,¹¹ R. Vilar,¹¹ T. Vine,³⁰ M. Vogel,³⁶ I. Volobouev^q,²⁸ G. Volpi,⁴⁵ F. Würthwein,⁹ P. Wagner,⁴⁴ R.G. Wagner,² R.L. Wagner,¹⁷ J. Wagner,²⁶ W. Wagner,²⁶ R. Wallny,⁸ S.M. Wang,¹ A. Warburton,³³ D. Waters,³⁰ M. Weinberger,⁵² W.C. Wester III,¹⁷ B. Whitehouse,⁵⁵ D. Whiteson^e,⁴⁴ A.B. Wicklund,² E. Wicklund,¹⁷ G. Williams,³³ H.H. Williams,⁴⁴ P. Wilson,¹⁷ B.L. Winer,³⁸ P. Wittich^g,¹⁷ S. Wolbers,¹⁷ C. Wolfe,¹³ T. Wright,³⁴ X. Wu,²⁰ S.M. Wynne,²⁹ A. Yagil,⁹ K. Yamamoto,⁴⁰ J. Yamaoka,⁵¹ T. Yamashita,³⁹ C. Yang,⁵⁹ U.K. Yang^m,¹³ Y.C. Yang,²⁷ W.M. Yao,²⁸ G.P. Yeh,¹⁷ J. Yoh,¹⁷ K. Yorita,¹³ T. Yoshida,⁴⁰ G.B. Yu,⁴⁸ I. Yu,²⁷ S.S. Yu,¹⁷ J.C. Yun,¹⁷ L. Zanello,⁵⁰ A. Zanetti,⁵³ I. Zaw,²² X. Zhang,²⁴ Y. Zheng^b,⁸ and S. Zucchelli⁵

(CDF Collaboration*)

¹*Institute of Physics, Academia Sinica, Taipei, Taiwan 11529, Republic of China*

²*Argonne National Laboratory, Argonne, Illinois 60439*

³*Institut de Fisica d'Altes Energies, Universitat Autònoma de Barcelona, E-08193, Bellaterra (Barcelona), Spain*

⁴*Baylor University, Waco, Texas 76798*

⁵*Istituto Nazionale di Fisica Nucleare, University of Bologna, I-40127 Bologna, Italy*

⁶*Brandeis University, Waltham, Massachusetts 02254*

⁷*University of California, Davis, Davis, California 95616*

⁸*University of California, Los Angeles, Los Angeles, California 90024*

⁹*University of California, San Diego, La Jolla, California 92093*

¹⁰*University of California, Santa Barbara, Santa Barbara, California 93106*

¹¹*Instituto de Fisica de Cantabria, CSIC-University of Cantabria, 39005 Santander, Spain*

¹²*Carnegie Mellon University, Pittsburgh, PA 15213*

¹³*Enrico Fermi Institute, University of Chicago, Chicago, Illinois 60637*

¹⁴*Comenius University, 842 48 Bratislava, Slovakia; Institute of Experimental Physics, 040 01 Kosice, Slovakia*

¹⁵*Joint Institute for Nuclear Research, RU-141980 Dubna, Russia*

¹⁶*Duke University, Durham, North Carolina 27708*

¹⁷*Fermi National Accelerator Laboratory, Batavia, Illinois 60510*

¹⁸*University of Florida, Gainesville, Florida 32611*

¹⁹*Laboratori Nazionali di Frascati, Istituto Nazionale di Fisica Nucleare, I-00044 Frascati, Italy*

²⁰*University of Geneva, CH-1211 Geneva 4, Switzerland*

²¹*Glasgow University, Glasgow G12 8QQ, United Kingdom*

²²*Harvard University, Cambridge, Massachusetts 02138*

²³*Division of High Energy Physics, Department of Physics,*

University of Helsinki and Helsinki Institute of Physics, FIN-00014, Helsinki, Finland

²⁴*University of Illinois, Urbana, Illinois 61801*

- ²⁵The Johns Hopkins University, Baltimore, Maryland 21218
- ²⁶Institut für Experimentelle Kernphysik, Universität Karlsruhe, 76128 Karlsruhe, Germany
- ²⁷Center for High Energy Physics: Kyungpook National University, Taegu 702-701, Korea; Seoul National University, Seoul 151-742, Korea; SungKyunKwan University, Suwon 440-746, Korea; Korea Institute of Science and Technology Information, Daejeon, 305-806, Korea; Chonnam National University, Gwangju, 500-757, Korea
- ²⁸Ernest Orlando Lawrence Berkeley National Laboratory, Berkeley, California 94720
- ²⁹University of Liverpool, Liverpool L69 7ZE, United Kingdom
- ³⁰University College London, London WC1E 6BT, United Kingdom
- ³¹Centro de Investigaciones Energeticas Medioambientales y Tecnologicas, E-28040 Madrid, Spain
- ³²Massachusetts Institute of Technology, Cambridge, Massachusetts 02139
- ³³Institute of Particle Physics: McGill University, Montréal, Canada H3A 2T8; and University of Toronto, Toronto, Canada M5S 1A7
- ³⁴University of Michigan, Ann Arbor, Michigan 48109
- ³⁵Michigan State University, East Lansing, Michigan 48824
- ³⁶University of New Mexico, Albuquerque, New Mexico 87131
- ³⁷Northwestern University, Evanston, Illinois 60208
- ³⁸The Ohio State University, Columbus, Ohio 43210
- ³⁹Okayama University, Okayama 700-8530, Japan
- ⁴⁰Osaka City University, Osaka 588, Japan
- ⁴¹University of Oxford, Oxford OX1 3RH, United Kingdom
- ⁴²University of Padova, Istituto Nazionale di Fisica Nucleare, Sezione di Padova-Trento, I-35131 Padova, Italy
- ⁴³LPNHE, Universite Pierre et Marie Curie/IN2P3-CNRS, UMR7585, Paris, F-75252 France
- ⁴⁴University of Pennsylvania, Philadelphia, Pennsylvania 19104
- ⁴⁵Istituto Nazionale di Fisica Nucleare Pisa, Universities of Pisa, Siena and Scuola Normale Superiore, I-56127 Pisa, Italy
- ⁴⁶University of Pittsburgh, Pittsburgh, Pennsylvania 15260
- ⁴⁷Purdue University, West Lafayette, Indiana 47907
- ⁴⁸University of Rochester, Rochester, New York 14627
- ⁴⁹The Rockefeller University, New York, New York 10021
- ⁵⁰Istituto Nazionale di Fisica Nucleare, Sezione di Roma 1, University of Rome "La Sapienza," I-00185 Roma, Italy
- ⁵¹Rutgers University, Piscataway, New Jersey 08855
- ⁵²Texas A&M University, College Station, Texas 77843
- ⁵³Istituto Nazionale di Fisica Nucleare, University of Trieste/ Udine, Italy
- ⁵⁴University of Tsukuba, Tsukuba, Ibaraki 305, Japan
- ⁵⁵Tufts University, Medford, Massachusetts 02155
- ⁵⁶Waseda University, Tokyo 169, Japan
- ⁵⁷Wayne State University, Detroit, Michigan 48201
- ⁵⁸University of Wisconsin, Madison, Wisconsin 53706
- ⁵⁹Yale University, New Haven, Connecticut 06520
- (Dated: August 22, 2007 Draft V2.21)

We report on a search for narrow-width particles decaying to a top and antitop quark pair. The data set used in the analysis corresponds to an integrated luminosity of 680 pb^{-1} collected with the Collider Detector at Fermilab in Run II. We present 95% confidence level upper limits on the cross section times branching ratio. Assuming a specific topcolor-assisted technicolor production model, the leptophobic Z' with width $\Gamma_{Z'} = 0.012M_{Z'}$, we exclude the mass range $M_{Z'} < 725 \text{ GeV}/c^2$ at the 95% confidence level.

PACS numbers: 14.70.Pw, 13.85.Rm

*With visitors from ^aUniversity of Athens, 15784 Athens, Greece, ^bChinese Academy of Sciences, Beijing 100864, China, ^cUniversity of Bristol, Bristol BS8 1TL, United Kingdom, ^dUniversity Libre de Bruxelles, B-1050 Brussels, Belgium, ^eUniversity of California, Irvine, Irvine, CA 92697, ^fUniversity of California Santa Cruz, Santa Cruz, CA 95064, ^gCornell University, Ithaca, NY 14853, ^hUniversity of Cyprus, Nicosia CY-1678, Cyprus, ⁱUniversity Col-

lege Dublin, Dublin 4, Ireland, ^jUniversity of Edinburgh, Edinburgh EH9 3JZ, United Kingdom, ^kUniversity of Heidelberg, D-69120 Heidelberg, Germany, ^lUniversidad Iberoamericana, Mexico D.F., Mexico, ^mUniversity of Manchester, Manchester M13 9PL, England, ⁿNagasaki Institute of Applied Science, Nagasaki, Japan, ^oUniversity de Oviedo, E-33007 Oviedo, Spain, ^pQueen Mary's Col-

The discovery of the top quark in 1995 at Fermilab [1] concluded a long search which occupied particle physicists for about two decades. Nevertheless, a decade after the top quark discovery there is still much to investigate about this massive but fundamental particle. There are several ways in which new physics can make an appearance through the top quark. The large mass in particular suggests that the top quark may play a special role in the dynamics of electroweak symmetry breaking and act as a powerful probe in this physics sector.

Among the technicolor scenarios, [2] predicts the existence of a heavy meson η_T produced in gluon-gluon interactions ($gg \rightarrow \eta_T \rightarrow t\bar{t}$). Topcolor models were investigated even before the actual discovery of the top [3], and then extended to topcolor assisted technicolor [4]. These scenarios account for the spontaneous breaking of electroweak symmetry by introducing new strong dynamics, which would explain the large top quark mass. An $SU(3) \times SU(1)$ residual global symmetry below 1 TeV predicts the existence of new particles like “topgluons” and a color singlet vector particle (Z') which couples primarily to the third quark generation. The existence of a narrow leptophobic Z' decaying to $t\bar{t}$ has been predicted in [5] and searched for in Tevatron Run I data [6].

Other $t\bar{t}$ production mechanisms can be found in universal extra dimensions theories. For example [7] investigated a standard model in 5+1 dimensions, where a series of narrow resonances decay to $t\bar{t}$ final states.

In this Letter, we present a search for narrow resonances decaying to $t\bar{t}$ by looking for an anomalous peak in the $t\bar{t}$ invariant mass distribution. The search algorithm was developed before looking at the data and optimized for signal from a leptophobic Z' decay. At the Tevatron, the Z' resonance can be produced via $q\bar{q}$ annihilation. The standard model (SM) predicts that the top quark decays more than 99% of the time into a Wb pair and then the W can decay either leptonically ($BR = 32.4\%$) or hadronically ($BR = 67.6\%$) [8].

The Collider Detector at Fermilab II (CDFII) [9] is an azimuthally and forward-backward symmetric apparatus designed to study $p\bar{p}$ collisions at $\sqrt{s} = 1.96$ TeV at the Tevatron. The detector has a charged particle tracking system [10] in a 1.4 T magnetic field directed parallel to the proton beam direction. This system consists of a silicon microstrip detector, which covers the radial range from 1.35 cm to 28 cm, and an open-cell drift chamber in the radial range from 40 cm to 137 cm. Outside the tracking system are the electromagnetic and hadronic calorimeters, with projective segmentation in η - ϕ [11]. A

set of drift chambers and scintillation counters detects muons in the central region ($|\eta| < 1$). The beam luminosity is determined by measuring the inelastic $p\bar{p}$ collision rate with gas Cherenkov detectors [12] located in the $3.7 < |\eta| < 4.7$ region.

We search for events in which one W boson decays hadronically and one leptonically. The partonic final state for this decay channel is $\ell\nu_\ell b\bar{b}q\bar{q}'$ ($\ell=e, \mu$), therefore the final state events have one high momentum charged lepton, large missing transverse energy (\cancel{E}_T) [11] due to the undetected neutrino, and four jets from the quarks' parton shower and hadronization processes (“lepton+jets” channel).

The data sample for this analysis has been collected using high- p_T triggers for electrons and muons [9]. The offline selection requires an electron (or muon) candidate with $E_T(p_T) > 20$ GeV contained in the central detector region. A jet is defined as an energy cluster in the calorimeter and is reconstructed using a fixed cone algorithm with a cone of radius 0.4 in $\eta - \phi$ space. Following the procedure described in [13], energies and \cancel{E}_T are corrected to account for inhomogeneities in the detector response and multiple $p\bar{p}$ collisions in an event. After these corrections we select events containing at least 4 jets with $|\eta| < 2$ and $E_T > 15$ GeV, and with $\cancel{E}_T > 20$ GeV. Jets originating from the hadronization of b quarks are identified (b -tagged), with about 40% efficiency, by reconstructing their displaced vertices [14]. The tagging information is not used for event selection, but only to reduce jet combinatorics during event reconstruction.

Standard model processes that result in the same final state as the resonance are backgrounds to this search. The dominant components are: W boson production in association with jets (W +jets), $t\bar{t}$ production, multi-jet events where a jet is mis-identified as a charged lepton and missing energy is generated by jet energy mismeasurement, and diboson production (WW, WZ, ZZ) with extra jets from initial and final state radiation (ISR, FSR). The expected contributions in a data set corresponding to an integrated luminosity of 680 pb^{-1} are presented in Table I. Standard model $t\bar{t}$ and diboson expec-

TABLE I: Expected number of events from standard model processes in a dataset corresponding to an integrated luminosity of 680 pb^{-1} of data, assuming the null hypothesis. The observed number of events on data is 450.

Background	number of events
SM $t\bar{t}$	199 ± 24
diboson	14 ± 1
multi-jet	22 ± 10
$W(\rightarrow \ell\bar{\nu}_\ell) + 4j$	215 ± 30

lege, University of London, London, E1 4NS, England, ^qTexas Tech University, Lubbock, TX 79409, ^rIFIC(CSIC-Universitat de Valencia), 46071 Valencia, Spain,

tations are calculated according to their theoretical cross sections [15, 16] and their acceptances estimated from

Monte Carlo simulations (see later). The quoted uncertainties include the uncertainties on the theoretical cross sections, integrated luminosity, and acceptances. Given the lack of precise theoretical predictions for W +jets and multi-jet production cross sections, the contributions from these backgrounds listed in Table I are obtained by constraining the total numbers to add up to the 450 events observed in data. The multi-jets to W +jets ratio in this sample is fixed at 10%, which is consistent with an estimate obtained in a previous CDF analysis [9]. The quoted uncertainties for these two backgrounds account for both the Poisson statistical uncertainty on the total number of observed events and the uncertainties on the $t\bar{t}$ and diboson predictions.

The signature for top-quark-pair resonant production is a peak in the invariant mass spectrum of the $t\bar{t}$ pair ($M_{t\bar{t}}$), over a smooth background from the standard model contributions. In the mass range investigated here, all of the standard model backgrounds fall smoothly with increasing $M_{t\bar{t}}$, reflecting the parton distribution functions of the incoming protons and antiprotons.

The resolution on the $t\bar{t}$ invariant mass is limited by the uncertainty on the jet energy and by the unmeasured longitudinal momentum of the neutrino. The approach adopted here is to use a matrix element technique [17] to reconstruct $M_{t\bar{t}}$ for an event. We integrate the matrix-element for standard model $t\bar{t}$ production over unmeasured quantities, convoluted with detector resolution functions for the jet energies. The matrix element implemented for the event reconstruction is the standard model leading order $t\bar{t}$ production and decay, $q\bar{q}(gg) \rightarrow t\bar{t} \rightarrow W^+bW^-\bar{b} \rightarrow q\bar{q}'b\ell\nu_\ell\bar{b}$, and it is used to derive the value of $M_{t\bar{t}}$ in the same way for events in simulated samples and in data.

The *a priori* probability density for producing a $t\bar{t}$ parton-level final state, $\pi_{\text{part}}(\{\vec{p}\})$, relative to other $t\bar{t}$ final states, is the normalized differential cross section

$$\begin{aligned} \pi_{\text{part}}(\{\vec{p}\}) & \prod_i d^3\vec{p}_i = \\ & = \frac{1}{\sigma} \int_0^1 \int_0^1 dz_a dz_b f_k(z_a) f_l(z_b) d\sigma_{kl}(\{\vec{p}\}, z_a \vec{P}, z_b \vec{P}), \end{aligned}$$

where f_k (f_l) are the proton (antiproton) parton distribution functions, $d\sigma_{kl}$ the $t\bar{t}$ differential cross section, \vec{P} (\vec{P}) the proton (antiproton) momentum and $\{\vec{p}\}$ the set of six final state three-momenta. Indices k, l cover the parton types in the proton and antiproton respectively, and a sum over both indices is implied. The *a priori* probability density for the parton level final state $\{\vec{p}\}$ and the measured jet quantities $\{\vec{j}\}$ is given by the product

$$\begin{aligned} \pi_{\text{part,jets}}(\{\vec{p}\}, \{\vec{j}\}) & = \\ & = \pi_{\text{part}}(\{\vec{p}\}) \cdot T(\vec{j}_1|\vec{p}_1) \cdot T(\vec{j}_2|\vec{p}_2) \cdot T(\vec{j}_3|\vec{p}_3) \cdot T(\vec{j}_4|\vec{p}_4), \end{aligned}$$

where $T(\vec{j}|\vec{p})$ denotes the parton to jet transfer function, i.e. the probability that a parton of momentum \vec{p} is measured as a jet of momentum \vec{j} . Transfer functions are parametrized in $|\eta|$ and momentum of the jet, and are derived from Monte Carlo simulated (PYTHIA) [18] events. Different sets of transfer functions are adopted for b -quarks and lighter quarks. No transfer function is used for the charged lepton given its negligible momentum uncertainty. Also, the \cancel{E}_T measurement is not used to constrain the neutrino transverse momentum.

From $\pi_{\text{part,jets}}(\{\vec{p}\}, \{\vec{j}\})$ we build $P(\{\vec{p}\}|\{\vec{j}\})$, the probability density for the parton momenta $\{\vec{p}\}$, given the observed quantities $\{\vec{j}\}$. From this distribution we derive probability distributions for the new variable, $M_{t\bar{t}}$, which is a function of the parton level quantities $\{\vec{p}\}$, by calculating $P_f(x|\{\vec{j}\}) = \int P(\{\vec{p}\}|\{\vec{j}\}) \cdot \delta(x - M_{t\bar{t}}(\{\vec{p}\})) d\{\vec{p}\}$. Having an event probability distribution for $M_{t\bar{t}}$ we choose the mean as the reconstructed value for that event, since Monte Carlo simulations showed it to be the best single value $M_{t\bar{t}}$ estimator. However, given that we do not know which jet matches which parton we also sum over all possible permutations before extracting the mean. If the event contains jets identified as originating from b -quarks we sum only over permutations with b -tagged jets assigned to b -quark partons.

To produce the $M_{t\bar{t}}$ templates we apply the reconstruction algorithm to each signal and background sample. The PYTHIA [18] generator was used to simulate both the Z' vector resonant production ($M_t = 175 \text{ GeV}/c^2$) and $t\bar{t}$ events. ALPGEN [19] was used for the simulation of the W boson plus parton production, with HERWIG [20] used to model parton showers. All generated events are passed through the CDF detector simulation. The multi-jet background template was obtained using CDF II data.

To allow direct comparison with the Tevatron Run I results [6] we choose a resonance width $\Gamma_{Z'} = 0.012 M_{Z'}$; however, the measured signal cross section upper limits are insensitive to width values up to $\Gamma_{Z'} \approx 0.05 M_{Z'}$. The algorithm shows an intrinsic resolution on $M_{t\bar{t}}$ of about $25 \text{ GeV}/c^2$ when applied to standard model $t\bar{t}$ events, in case of correct partons to jet association. When applied to resonance samples the mass is still correctly reconstructed in the case of proper parton-jet assignment; however, incorrect parton-jet assignment leads to a low tail in the reconstructed mass distribution as explained in Fig. 1. The spectra plotted are restricted to the search region ($M_{t\bar{t}} > 400 \text{ GeV}/c^2$) in which the standard model sources fall off exponentially in $M_{t\bar{t}}$.

To derive the posterior probability for $\sigma(p\bar{p} \rightarrow Z') \cdot BR(Z' \rightarrow t\bar{t})$ (we will refer to it simply as “signal cross section”) given the observed $M_{t\bar{t}}$ spectrum, we build the likelihood $\mathcal{L}(\vec{n}|\sigma, \vec{\nu}) = \prod_{i \in \{\text{bins}\}} e^{-\mu_i} \mu_i^{n_i} / n_i!$. This is the prior probability of observing \vec{n} , where n_i is the number of observed events in $M_{t\bar{t}}$ mass bin i , $\mu_i = \sigma_s A_s T_{s_i} + \sum_j N_j T_{j_i}$ is the number of expected

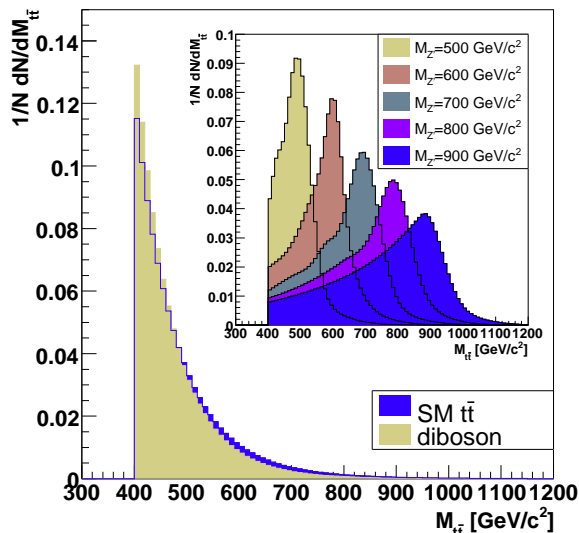


FIG. 1: Reconstructed $M_{t\bar{t}}$ distributions for two simulated standard model backgrounds. We plot the samples with the “hardest” ($t\bar{t}$) and the “softest” (diboson) spectrum (normalized to unity); all the others lie in between. The inset shows the reconstructed $M_{t\bar{t}}$ distributions for five signal samples.

events in the same bin, σ_s is the assumed signal cross section, A_s is the acceptance, N_j is the contribution from the j^{th} background and T_{si} , T_{ji} is the content of the i^{th} bin of the normalized signal and background templates, respectively. The contributions from standard model $t\bar{t}$ and dibosons are weighted as in Table I, while the contributions due to W +jets and multi-jets are rescaled to account for the presence of signal and still match the total number of events observed ($N_{W+\text{jets}} + N_{\text{multi-jet}} = N_{\text{data}} - N_{\text{signal}} - N_{t\bar{t}} - N_{\text{diboson}}$). If one uses a flat prior distribution for the signal cross section and integrates over the nuisance parameters $\vec{\nu}$ (background contributions and signal acceptance) then Bayes’ theorem gives the posterior probability density $P(\sigma|\vec{n})$.

The posterior probability density is used to define upper limits at any given confidence level (CL), together with the most likely value which is regarded as the measured cross section. This procedure is repeated for 10 resonance masses from $450 \text{ GeV}/c^2$ to $900 \text{ GeV}/c^2$ and 95% CL upper limits are established.

As mentioned previously, uncertainties on template weighting are incorporated in the prior probability by means of the prior densities of the nuisance parameters. In this way the marginalized posterior probability density for the signal cross section includes the acceptance and cross section uncertainties. However, the relative contribution of multi-jet and W +jet events has been kept fixed at 10%. To evaluate the impact of the uncertainty on this ratio, the multi-jet component has been either set to zero or increased by a factor of three, in each case yielding negligible change on the cross section posterior

distribution. This is because after the event selection the W +jet and multi-jet $M_{t\bar{t}}$ spectra are very similar above $400 \text{ GeV}/c^2$, as shown in Fig. 1. We assume a 10% acceptance uncertainty for all the resonant $t\bar{t}$ signals.

Other sources of systematic uncertainties can affect both the acceptances and the templates. These “shape systematics” are due to the imperfect knowledge in the modeling of (1) jet energy scale, (2) ISR and FSR, (3) the Q^2 scale for W +jets production, and (4) parton distribution functions (PDF). To account for these uncertainties we convolute the cross section posterior probability with a Gaussian, whose width is estimated from a new set of templates and acceptances corresponding to a $\pm 1\sigma$ change for each systematic. The result of this convolution smears the cross section posterior, pushing the upper limits to higher cross section values. For a resonance of mass $M_{Z'} = 700 \text{ GeV}/c^2$ the uncertainties on the jet energy scale, initial and final state radiation, $W - Q^2$ scale translate into a relative increase of the expected upper limits of 5%, 5%, 2% and 2% respectively, for an overall impact of about 10%. The uncertainty due to the choice of the PDFs turned out to be negligible.

In the data sample used for this analysis, 450 events passed our event selection requirements, and 302 of them are found in the search region $M_{t\bar{t}} > 400 \text{ GeV}/c^2$. The $M_{t\bar{t}}$ data spectrum is shown in Fig. 2, together with the background expectations (above $400 \text{ GeV}/c^2$) based on Monte Carlo studies. In order to establish an *a priori* sensitivity of the reconstruction algorithm we generated 1000 simulated experiments in the null hypothesis and extracted, for each mass point, the 95% CL expected upper limit, defined as the median of the upper limits distribution. We also calculated the central 1σ and 2σ frequentist coverage bands.

In the data, the posterior probability distributions for the signal cross section show no evidence of resonant $t\bar{t}$ production. The predicted and observed upper limits at 95% CL are shown in Fig. 3, together with the theoretical prediction for the cross section as a function of mass in the leptophobic Z' model (with $\Gamma_{Z'} = 0.012 M_{Z'}$) [5]. Based on this model we exclude a leptophobic topcolor resonance candidate with a mass of $725 \text{ GeV}/c^2$ or less.

In conclusion, we performed a search for a narrow heavy resonance decaying into $t\bar{t}$ in the lepton+jets channel using 680 pb^{-1} of CDF Run 2 data. We set upper limits on the production cross section times branching ratio at the 95% CL. For one leptophobic topcolor production mechanism we exclude masses up to $725 \text{ GeV}/c^2$, extending significantly the Run I limit of $560 \text{ GeV}/c^2$ [6].

We thank the Fermilab staff and the technical staffs of the participating institutions for their vital contributions. This work was supported by the U.S. Department of Energy and National Science Foundation; the Italian Istituto Nazionale di Fisica Nucleare; the Ministry of Education, Culture, Sports, Science and Technology of Japan; the Natural Sciences and Engineering Research

Council of Canada; the National Science Council of the Republic of China; the Swiss National Science Foundation; the A.P. Sloan Foundation; the Bundesministerium für Bildung und Forschung, Germany; the Korean Science and Engineering Foundation and the Korean Research Foundation; the Science and Technology Facilities Council and the Royal Society, UK; the Institut National de Physique Nucleaire et Physique des Particules/CNRS; the Russian Foundation for Basic Research; the Comisión Interministerial de Ciencia y Tecnología, Spain; the European Community's Human Potential Programme; the Slovak R&D Agency; and the Academy of Finland.

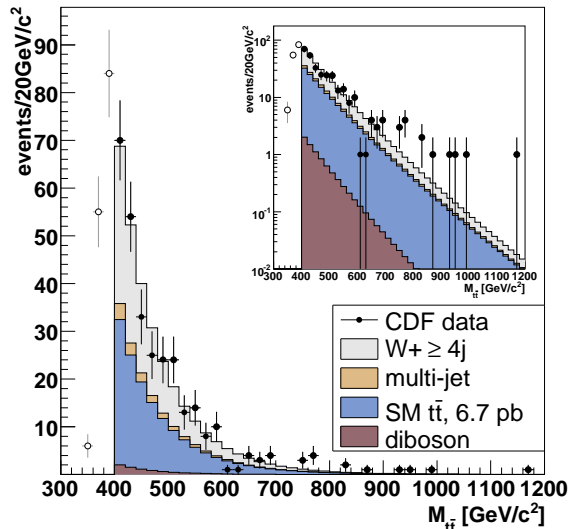


FIG. 2: The reconstructed $M_{t\bar{t}}$ spectrum (data) and the standard model prediction in the search region above $400 \text{ GeV}/c^2$. The inset shows the same distributions in logarithmic scale.

- [1] F. Abe *et al.* (CDF Collaboration), Phys. Rev. Lett. **74**, 2626 (1995); S. Abachi *et al.* (DØ Collaboration), *ibid.*, 2632 (1995).
- [2] E. Eichten and K. D. Lane, Phys. Lett. B **327**, 129 (1994).
- [3] C.T. Hill and S.J. Parke, Phys. Rev. D **49**, 4454 (1994).
- [4] C.T. Hill, Phys. Lett. B **345**, 483 (1995).
- [5] R.M. Harris, C.T. Hill, and S.J. Parke, arXiv:hep-ph/9911288, (1999).
- [6] A. Affolder *et al.* (CDF Collaboration), Phys. Rev. Lett. **85**, 2062 (2000); V. M. Abazov *et al.* (DØ Collaboration), Phys. Rev. Lett. **92**, 221801 (2004).
- [7] G. Burdman, B. A. Dobrescu, and E. Ponton, Phys. Rev. D **74**, 075008 (2006).
- [8] W.-M. F. Yao *et al.* (Particle Data Group), J. Phys. G Nucl. Part. Phys. **33**, 1 (2006).
- [9] D. Acosta *et al.* (CDF Collaboration), Phys. Rev. D **72**, 052003 (2005).
- [10] A. Sill (CDF Collaboration), Nucl. Instrum. Methods A

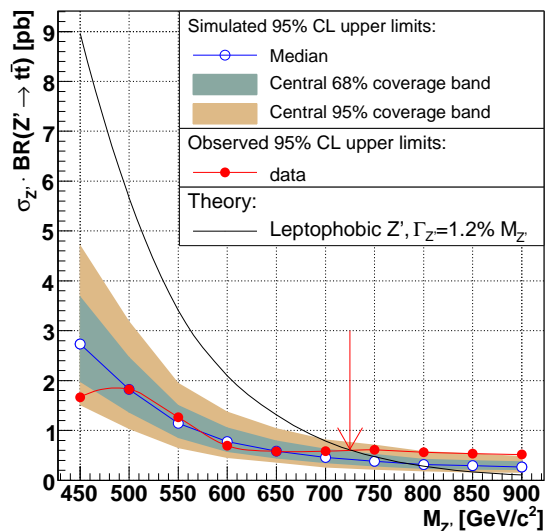


FIG. 3: Predicted and experimental 95% CL upper limits using data corresponding to 680 pb^{-1} of integrated luminosity, together with the leptophobic topcolor Z' cross section prediction. Dark and light areas define the 1σ and 2σ ranges for the expected limits. The arrow marks the mass upper limit.

447, 1 (2000). A. Affolder *et al.* (CDF Collaboration), Nucl. Instrum. Methods A **453**, 84 (2000). A. Affolder *et al.* (CDF Collaboration), Nucl. Instrum. Methods A **526**, 249 (2004).

- [11] CDF uses a (z, ϕ, θ) coordinate system with the z -axis in the direction of the proton beam; ϕ and θ are the azimuthal and polar angle respectively. The pseudorapidity is defined as $\eta = -\ln(\tan(\frac{\theta}{2}))$, and the transverse momentum and energy as $p_T = p \sin \theta$ and $E_T = E \sin \theta$ respectively. Missing transverse energy is defined as $\vec{E}_T = -\sum_i E_T^i \hat{n}_i$, where \hat{n}_i is a unit vector in the transverse plane that points from the beam-line to the i^{th} calorimeter tower.
- [12] D. Acosta *et al.*, Nucl. Instrum. Methods A **494**, 57 (2002).
- [13] A. Bhatti *et al.*, Nucl. Instrum. Methods A **566**, 375 (2006).
- [14] D. Acosta *et al.* (CDF Collaboration), Phys. Rev. D **71**, 052003 (2005).
- [15] N. Kidonakis and R. Vogt, Phys. Rev. D **68**, 114014 (2003); M. Cacciari *et al.*, J. High Energy Phys. **0404**, 068 (2004).
- [16] J. M. Campbell and R. K. Ellis, Phys. Rev. D **60**, 113006 (1999).
- [17] K. Kondo, J. Phys. Soc. Jap. **57**, 4126 (1988); **60**, 836 (1991); A. Abulencia *et al.* (CDF Collaboration), Phys. Rev. D **73**, 092002 (2006); V. M. Abazov *et al.* (DØ Collaboration), Phys. Rev. D **74**, 092005 (2006).
- [18] T. Sjostrand, P. Eden, C. Friberg, L. Lonnblad, G. Miu, S. Mrenna, and E. Norrbin, Comput. Phys. Commun. **135**, 238 (2001).
- [19] M. L. Mangano *et al.*, J. High Energy Phys. **0307**, 001 (2003).
- [20] G. Corcella *et al.*, J. High Energy Phys. **0101**, 010 (2001); hep-ph/0210213 (2002).